Journal of
Nanoscience and Nanotechnology
Vol. 9, 1496–1500, 2009

Metal Hydroxide and Metal Oxide Nanostructures from Metal Corrosion

Huanping Yang[1], Yun Ma[1], Zhenhua Ni[2], Zexiang Shen[1], Yuanping Feng[2], and Ting Yu[1,*]

[1] *Division of Physics and Applied Physics, School of Physical and Mathematical Sciences, Nanyang Technological University, 1 Nanyang Walk, Block 5, Singapore 637616*
[2] *Department of Physics, National University of Singapore, 2 Science Drive 3, Singapore 117542*

Unique metal hydroxide ($Co(OH)_2$ and $Mg(OH)_2$) and metal oxide (Co_3O_4 and MgO) nanosheet arrays have been successfully achieved on a large scale by simple metal corrosion process in deionized water at room temperature. The X-ray diffraction (XRD) and micro-Raman scattering investigations reveal the crystalline feature of the resulted nanosheets. The magnesium based nanosheet exhibits strong visible photoluminescence (PL) emission. The water wettability of cobalt based nanosheet has also been studied.

Keywords: Metal Oxide, Nanosheet Arrays, Corrosion.

1. INTRODUCTION

The morphology and dimension control is a critical issue in the current nanomaterials fabrication as both the properties and potential applications of these materials reply on their unique sizes and shapes.[1–8] Although many strategies have been developed for the controllable fabrication of nanostructures with various morphologies and dimensions, intensive efforts are required to seek even simpler and more efficient approaches for synthesis of nanomaterials with more promising potentials like low cost, high yield and large scale.[3,5,6] So far few works have demonstrated the successful synthesis of metal nanoboxes, nanocages and membranes by corrosion process,[9,10] "the damage of metal caused by reactions with its environment" as broadly defined, although it is generally undesirable.[11]

Cobalt hydroxides have attracted increasing attention as they can be used as additives of alkaline secondary batteries and as precursors of heterogeneous catalysts. Cobalt hydroxide films exhibit catalytic and reversible electrochromic properties.[12–14] Due to its potential applications in ceramic pigments, solid-state sensors, energy storage as intercalation compounds, rotatable magnets, heterogeneous catalysts, and electrochromic devices,[15–17] cobalt oxide becomes an important and promising *P*-type semiconductor. Meanwhile, many efforts have also been afforded on the fabrication of cobalt oxide nanostructures with various morphologies.[3,5,17–19]

Magnesium hydroxide as a flame retardant has been widely employed in many polymers, electric cables, building and decoration materials.[6] To date, different morphologies of $Mg(OH)_2$ materials, such as the needle-like, lamella-like, wire-like, rod-like have been prepared.[20] Magnesium oxide is a very important scientific and commercial material for use in catalysis,[21] toxic waste remediation,[22] or as additives in refractory, paint, and superconductor products.[23] Various MgO morphologies, for instance fibers, fishbone and fernlike nanostructures have been synthesized by different methods.[24–26]

In this work, we report on a simple method of fabricating cobalt and magnesium hydroxide and oxide nanosheet arrays via metal corrosion process in deionized water at room temperature and post-annealing process in vacuum at 150 °C. The water wettability of the cobalt hydroxide/oxide nanosheet film has also been investigated.

2. EXPERIMENTAL DETAILS

Experimentally, fresh cobalt foils (10 mm × 10 mm × 0.25 mm) and magnesium belts (10 mm × 5 mm × 0.25 mm) with purity of 99.9% (Aldrich) were used as starting materials for the growth of metal hydroxide and oxide. The polished and cleaned metal foils were fully immersed in deionized water (pH = 7.22). The corrosion process lasts 3 days. The corroded metals were subjected to a post-annealing process in vacuum (pressure = 10^{-2} Torr) at 150 °C for 5 hours. The surface morphologies of as-corroded and heated samples

*Author to whom correspondence should be addressed.

1533-4880/2009/9/1496/005 doi:10.1166/jnn.2009.C187

were examined by scanning electron microscopy (SEM) (JEOL JSM-6700F). The compositions were characterized by X-ray diffraction (XRD) (Bruker D8 with Cu K_α irradiation), micro-Raman spectroscopy (Witech CRM200, $\lambda_{laser} = 532$ nm) and photoluminescence (PL) spectroscopy (Renishaw inVia Raman system, $\lambda_{laser} = 325$ nm). The water wettability of cobalt hydroxide/oxide nanosheet films were studied by measuring the water contact angles (WCA) (First Ten Angstroms, FTA1000).

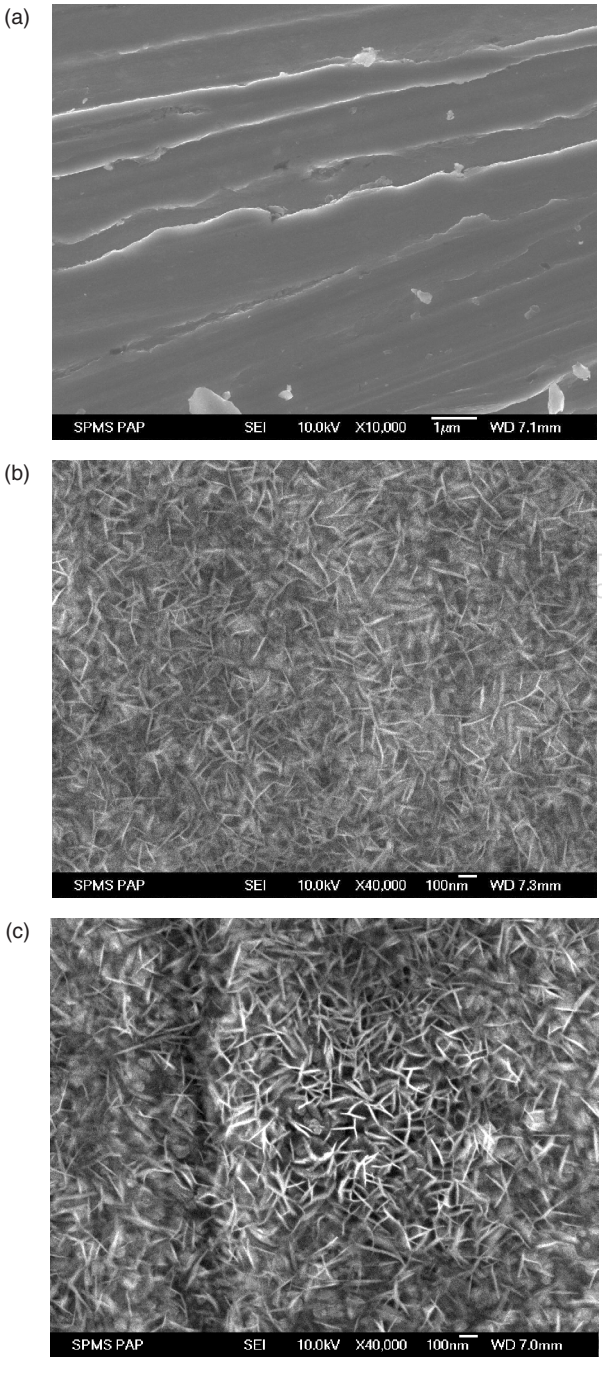

Fig. 1. SEM images of the top surfaces of (a) Co foil, (b) 3 day-corroded sample and (c) the corroded sample after post-annealing at 150 °C for 5 hours at pressure of 10^{-2} Torr.

3. RESULTS AND DISCUSSION

Figure 1 shows the SEM images of pure cobalt foil (see Fig. 1(a)), as-corroded for 3 days (see Fig. 1(b)) and annealed at 150 °C for 5 h under vacuum (see Fig. 1(c)) samples, respectively. As shown in Figure 1(b), the cobalt foil surface was surprisingly populated with vertically aligned nanosheet arrays after 3-day corrosion process in deionized water at room temperature. The nanosheets are slightly curved and approximately 10 nm in width and 120 nm in length. No much lateral growth of the nanosheets was observed in the annealed sample comparing with the as-corroded. However, the height of the nanosheets obviously increases for annealed sample which results in the large increase of the pores as well as the surface roughness.

Figure 2 shows the Raman spectra of surfaces of as-corroded and annealed cobalt-based samples. The Lorentzian curve fitting of the spectrum of as-corroded sample resolved four peaks in the range of 300–750 cm^{-1}. The peaks locating at 458 cm^{-1} and 526 cm^{-1} correspond to the cobalt hydroxide[27] while the peaks locating at 483 cm^{-1} and 689 cm^{-1} match well with the Raman vibrational modes of cobalt oxide.[28] It was noted that both the Raman modes of the hydroxide and oxide show a red-shift. This can be attributed to the nanoscale size of the nanosheets. It can be clearly seen that the cobalt oxide is the dominant phase in the annealed sample, implying the readily transformation from hydroxide to oxide triggered by the post-annealing process. The Raman scattering investigations indicate the nanosheets formed by the corrosion of cobalt foil is the mixture of crystalline cobalt hydroxide and cobalt oxide. The post thermal treatment is able to transform the hydroxide into oxide easily.

Figure 3 shows SEM images of the pure magnesium foil (Fig. 3(a)), as-corroded (3 days) (Fig. 3(b)) and the annealed (150 °C/5 h in vacuum) (Fig. 3(c)) samples.

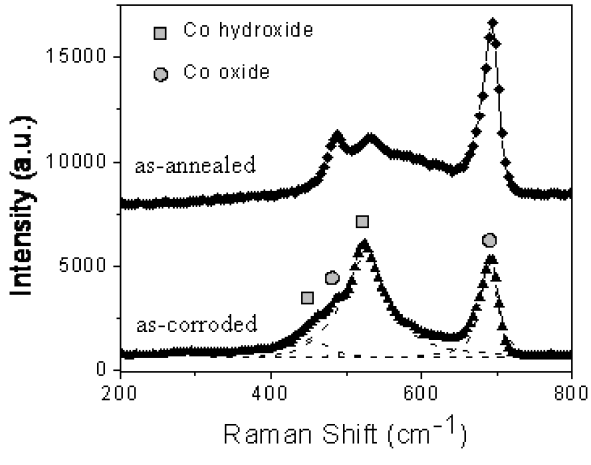

Fig. 2. Raman spectra of the as-corroded and as-annealed Co-based nanosheets. The dash lines indicate the Lorentzian curve fitting results.

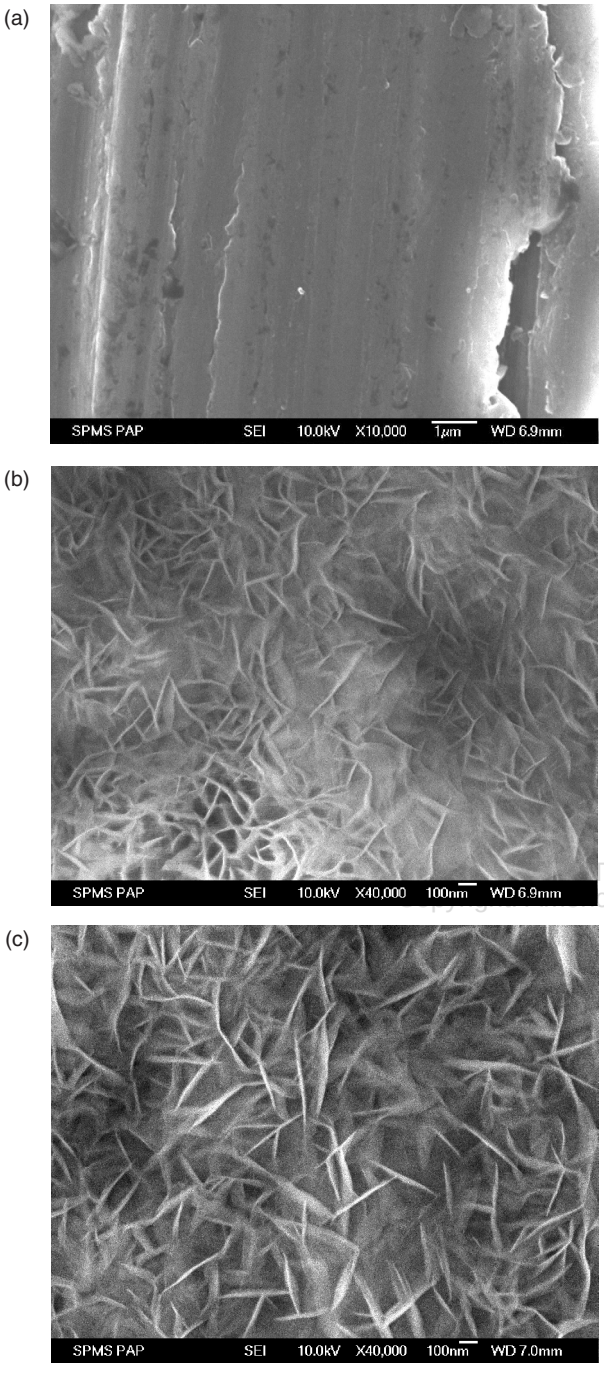

Fig. 3. SEM images of the top surfaces of (a) Mg foil, (b) 3 day-corroded sample and (c) the corroded sample after post-annealing at 150 °C for 5 hours at pressure of 10^{-2} Torr.

Similarly, the nanosheet arrays were generated by the corrosion process and characterized with more pores as well as high roughness after the annealing. Deviating from cobalt hydroxide and oxide nanosheets, the magnesium-based nanosheets exhibit larger dimensions, approximately 15 nm in width and 400 nm in length. This may be due to the higher chemical activity of magnesium comparing with cobalt.

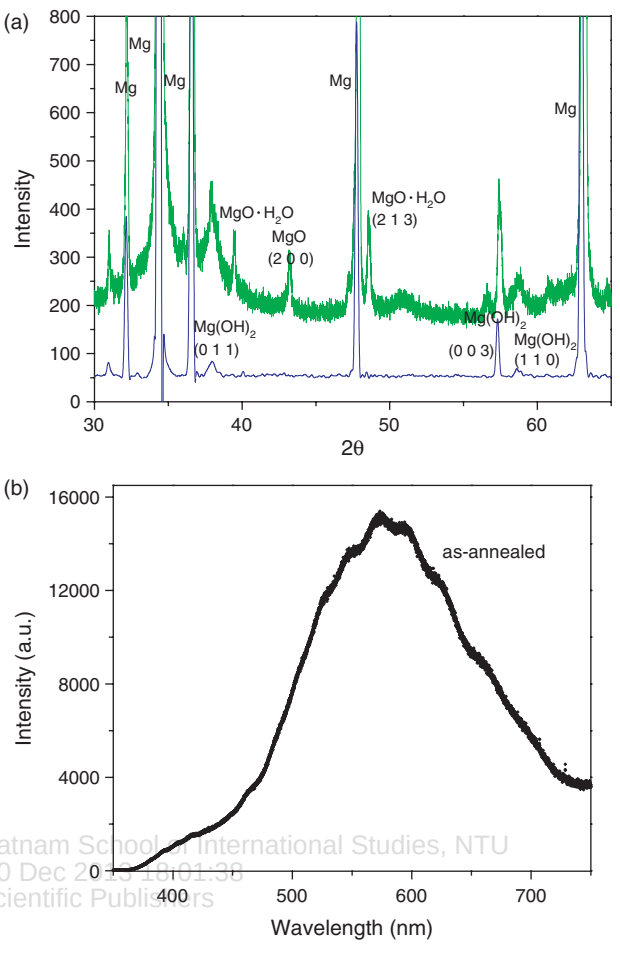

Fig. 4. (a) XRD patterns of the as-corroded (bottom) and the as-annealed (top) Mg-based nanosheets, (b) PL spectrum of the as-annealed sample.

Figure 4(a) shows the XRD patterns of the as-corroded and the heated magnesium based samples. Besides the very sharp peaks from metal substrate,[29] the appearance of the $Mg(OH)_2$ peaks[29] indicates the crystal structural and composition features of the nanosheets on the surface of the corroded sample. After the post-annealing process, the MgO peaks[29] present, implying the formation of the crystalline MgO. Figure 4(b) shows the photoluminescence (PL) spectrum of the annealed sample. A broad PL band centered at around 575 nm presents in both the as-corroded (not shown) and the annealed samples. The PL emission of the MgO nanostructures covers most of visible range from 383 nm to 721 nm.[30–32] The variety of the PL emission of MgO nanostructures could be attributed to the various structural defects associated with the oxygen vacancies, Mg vacancies and interstitials, which could induce new energy levels within the band gap of the MgO nanocrystals.[30–32]

Figure 5 shows the optical photographs of water droplet shape on as-corroded and as-annealed cobalt hydroxide/oxide nanosheet arrays. The water wettability was

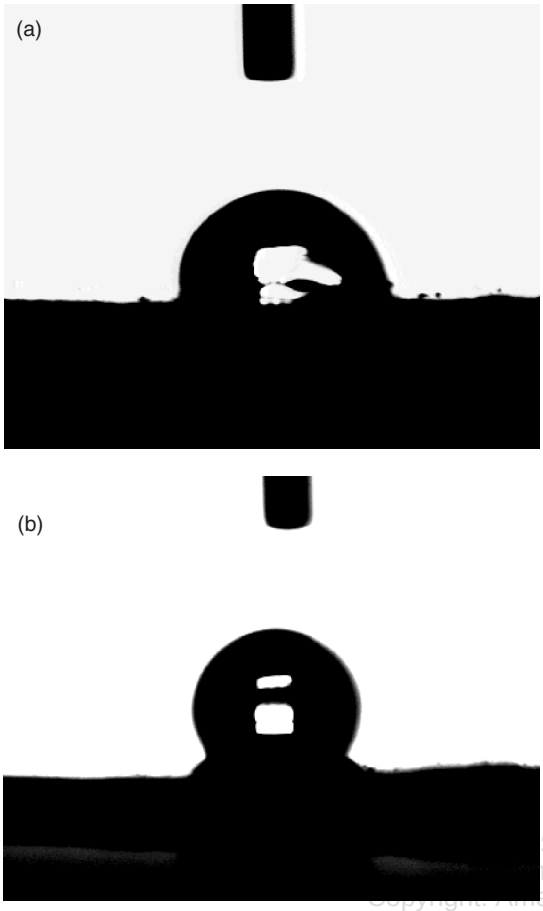

Fig. 5. Photographs of water droplet shape on (a) as-corroded and (b) as-annealed Co-based nanosheet arrays.

evaluated by the water contact angle (CA) measurement. A semi-spherical water droplet with a CA of 85° was observed, indicating the hydrophilic property of the as-corroded sample. After thermal treatment, the CA increases to 125°, implying the hydrophobic feature. The transition between hydrophilicity to hydrophobicity could be due to the significant increase of the pores and surface roughness after the heating process.

The growth mechanism is temporarily explained by the metal corrosion theory, especially the fully immersed corrosion model. As reported, corrosion most commonly occurs when the O_2 in air is dissolved in a thin film of water on the surface of a metal, thereby picking up electrons from the cathode to from hydroxide ions that then migrate towards the anode.[11] For a specimen of metal that is totally immersed in water, the anodic and cathodic sites are not usually separate. All parts of the surface during corrosion could be anodic and cathodic alternately over a period of time. Any part of the surface corrodes at the same average rate as any other part of the surface. The accumulation of cations might lead to the corrosion products such as hydroxide and oxide precipitating and covering the whole surface. This causes the uniform growth of nanosheets (see Figs. 1 and 3). The drop off the pH values ($pH_{Co} = 6.53$ and $pH_{Mg} = 7.18$) also support the formation of hydroxide precipitation.

4. CONCLUSIONS

In summary, vertically aligned cobalt and magnesium hydroxide and oxide nanosheets have been synthesized using a rather simple metal corrosion process in deionized water at room temperature. XRD and micro-Raman scattering investigation indicate the crystalline structural features of these nanosheets. A strong visible PL emission from MgO nanosheets was observed. The water wettability of cobalt hydroxide/oxide nanosheet arrays could be readily tuned from hydrophilic to hydrophobic by post-annealing process, which results from the significant increase of the pores and surface roughness after the annealing.

References and Notes

1. Y. Yin, G. Zhang, and Y. Xia, *Adv. Funct. Mater.* 12, 293 (**2002**).
2. Y. Li, M. Sui, Y. Ding, G. Zhang, J. Zhuang, and C. Wang, *Adv. Mater.* 12, 818 (**2000**).
3. T. Yu, Y. W. Zhu, X. J. Xu, K. S. Yeong, Z. X. Shen, P. Chen, C. T. Lim, J. T. L. Thong, and C. H. Sow, *Small* 2, 80 (**2006**).
4. Y. W. Zhu, H. I. Elim, Y. L. Foo, T. Yu, Y. J. Liu, W. Ji, J. Y. Lee, Z. X. Shen, A. T. S. Wee, J. T. L. Thong, and C. H. Sow, *Adv. Mater.* 18, 587 (**2006**).
5. T. Yu, Y. W. Zhu, X. J. Xu, Z. X. Shen, P. Chen, C. T. Lim, J. T. L. Thong, and C. H. Sow, *Adv. Mater.* 17, 1595 (**2005**).
6. C. L. Yan, D. F. Xue, L. J. Zou, X. X. Yan, and W. Wang, *J. Cryst. Growth* 282, 448 (**2005**).
7. Z. W. Liu, C. K. Ong, T. Yu, and Z. X. Shen, *Appl. Phys. Lett.* 88, 053110 (**2006**).
8. T. Yu, X. Zhao, Z. X. Shen, Y. H. Wu, and W. H. Su, *J. Cryst. Growth* 268, 590 (**2004**).
9. Y. Ding and J. Erlebacher, *J. Am. Chem. Soc.* 125, 7772 (**2003**).
10. Y. J. Xiong, B. Wiley, J. Y. Chen, Z. Y. Li, Y. D. Yin, and Y. N. Xia, *Angew. Chem.* 44, 7913 (**2005**).
11. S. A. Bradford, Corrosion Control, 2nd edn., CASTI Publishing, Edmonton, Canada (**2001**), pp. 1–51.
12. K. Watanabe, T. Kikuoka, and N. Kumagai, *J. Appl. Electrochem.* 25, 219 (**1995**).
13. M. Dinamani and P. V. Kamath, *J. Appl. Electrochem.* 305, 1157 (**2000**).
14. N. Jozer, D. G. Chen, and T. Buyuklimanli, *Sol. Energy Mater. Sol. Cells* 52, 223 (**1998**).
15. T. He, D. Chen, X. Jiao, Y. Xu, and Y. Gu, *Langmuir* 20, 8408 (**2004**).
16. S. Takada, M. Fujii, and S. Kohiki, *Nano Lett.* 1, 379 (**2001**).
17. R. Xu and H. C. Zeng, *Langmuir* 20, 9780 (**2004**).
18. B. B. Lakshmi, C. J. Patrissi, and C. R. Martin, *Chem. Commun.* 9, 2544 (**1997**).
19. X. S. Shi, S. Han, R. J. Sanedrin, F. Zhou, and M. Selke, *Chem. Mater.* 14, 1897 (**2002**).
20. Y. Ding, G. T. Zhang, H. Wu, B. Hai, L. B. Wang, and Y. T. Qian, *Chem. Mater.* 13, 434 (**2001**).
21. S. H. C. Liang and I. D. Gay, *J. Catal.* 101, 293 (**1986**).
22. A. N. Copp, *Am. Ceram. Soc. Bull.* 74, 135 (**1995**).
23. P. D. Yang and C. M. Lieber, *Science* 273, 1836 (**1996**).
24. G. Kordas, *J. Mater. Chem.* 10, 1157 (**2000**).
25. Y. Q. Zhu, W. K. Hsu, W. Z. Zhou, M. H. Terrones, H. W. Kroto, and D. R. M. Walton, *Chem. Phys. Lett.* 347, 337 (**2001**).

26. Y. Q. Zhu, W. K. Hsu, W. Z. Zhou, M. H. Terrones, H. W. Kroto, and D. R. M. Walton, *J. Mater. Chem.* 14, 685 (**2004**).
27. Y. S. Li, K. Wang, P. X. He, B. X. Huang, and P. Kovacs, *J. Raman Spectrosc.* 30, 97 (**1999**).
28. V. G. Hadjievl, M. N. Iliev, and I. V. Vergilov, *J. Phys. C: Solid State Phys.* 21, L199 (**1988**).
29. Cu K α 1 λ :1.54060 the card numbers are: 35-0821; 87-0653; 02-1395.
30. J. Zhang and L. Zhang, *Chem. Phys. Lett.* 363, 293 (**2002**).
31. G. H. Rosenblatt, M. W. Rowe, G. P. Williams, Jr., and R. T. Williams, *Phys. Rev. B* 39, 10309 (**1989**).
32. H. W. Kim and S. H. Shim, *Chem. Phys. Lett.* 422, 165 (**2006**).

Received: 7 June 2007. Accepted: 30 November 2007.